Solar Phys (2007) 243: 171–191
DOI 10.1007/s11207-007-0450-0

Topological Aspects of Global Magnetic Field Reversal in the Solar Corona

R.C. Maclean · E.R. Priest

Received: 20 March 2007 / Accepted: 6 June 2007 / Published online: 31 July 2007

Abstract Every eleven years on average, the dipolar component of the Sun's global coronal magnetic field reverses in sign – a consequence of the sunspot cycle. In this paper we begin to investigate the complex changes in coronal structure during the reversal. We present a simplified model of the solar cycle containing six time-varying photospheric sources of magnetic field and analyse the evolution of the global coronal field using the technique of magnetic charge topology. Surprisingly, a sequence of seventeen topological changes takes place in the model between one solar minimum state and the next; many of the resultant topological configurations correspond to observable magnetic field structures in the real corona. We also show how descriptions of all the six-source topological states from the model can be built up in terms of combinations of simpler four-source states, providing a framework for future descriptions of even more complicated topological states.

1. Introduction

As a first-order approximation, the global magnetic field of the Sun is dipolar, with its magnetic axis aligned with the solar rotation axis. The sign of this global dipolar field undergoes a reversal on average every 11 years, in a process called the solar cycle (Babcock, 1961; Leighton, 1969).

In fact, the true average length of a complete cycle is 22 years. The polar field reverses for the following reasons. Starting just after solar minimum, a small fraction of the magnetic flux contained in sunspots cancels over the equator. As described by Joy's law, there is a tilt in

R.C. Maclean (✉)
Armagh Observatory, College Hill, Armagh BT61 9DG, Northern Ireland, UK
e-mail: rcm@arm.ac.uk

E.R. Priest
Institute of Mathematics, University of St Andrews, The North Haugh, St Andrews, Fife KY16 9SS, Scotland, UK
e-mail: eric@mcs.st-and.ac.uk

sunspot groups such that the leading sunspot polarity is usually closer to the equator than the following polarity, and so more of the flux from the leading polarities is cancelled than from the following polarities. Typically 70% of the active-region flux is cancelled locally within each active region (Martinez Pillet, Sainz Dalda, and van Driel-Gesztelyi, 2004). Moreover, when cancellation with adjacent active regions is accounted for (Schrijver and Zwaan, 2000), less than 1% of the following-polarity flux (which is oppositely signed to the preexisting polar flux) remains uncancelled. This flux is preferentially transported towards the poles by meridional circulation (Topka *et al.*, 1982; Wang, Nash, and Sheeley, 1989; Wang, Sheeley, and Nash, 1991; Wang, Sheeley, and Lean, 2002; Mackay, Priest, and Lockwood, 2002; Mackay and van Ballegooijen, 2006a, 2006b). There it cancels with the polar flux, eventually annihilating it 2 – 3 years after solar maximum, and continues to build up at the poles until a reversed dominant dipolar field has accumulated, bringing the system to the next solar minimum. The process just described takes on average 11 years; just after solar minimum, the signs of the leading and following polarities of the sunspots switch, and it takes another 11 years for the system to return to its original configuration.

This solar cycle, or sunspot cycle, has been known since the mid-nineteenth century (Schwabe, 1844). However, in this paper we aim to provide a new perspective on the structure and evolution of the global solar magnetic field as it goes through the reversal. An interesting simple axisymmetric model was proposed by Zhang and Low (2001), in which new magnetic field emerges at the solar equator into a preexisting dipolar field of opposite polarity. Their model shows that this emerging field can drive magnetic reconnection, which in turn makes the global field reverse when the ratio of preexisting to emerged flux becomes large enough. The ratio can be increased by the prereversal opening up of some parts of the field (interpreted as a coronal mass ejection), which can remove some preexisting flux from the system. Our aim is to generalise their axisymmetric treatment of the field by setting up a more realistic fully three-dimensional (3D) model.

We achieve this by analysing a simple model of the 3D magnetic topology (Brown and Priest, 1999a, 2001; Longcope, 2005) of the global solar field during the reversal process. The technique we use is called magnetic charge topology (Beveridge and Longcope, 2005). Calculating the topology of a magnetic field is a way to determine its structure by locating its magnetic null points and their associated field lines (spines, separatrix surfaces, and separators) that bound regions of different magnetic connectivity. These topological features are sometimes associated with the occurrence of magnetic reconnection (Priest, Longcope, and Heyvaerts, 2005; Wilmot-Smith, Hornig, and Priest, 2006; Hornig and Priest, 2003; Pontin, Hornig, and Priest, 2005).

The paper is ordered as follows: Section 2 gives the details of the six-source fully 3D topological model. The model evolves through several distinct topological stages, which are described in detail in Section 3. Implications for the real solar cycle are discussed in Section 4, where we also summarise our results and consider how this work could be extended in future.

2. Model Design and Justification

The model consists of six point magnetic flux sources on the surface of a sphere. We model the entire global coronal magnetic field using the Green's function technique of Maclean *et al.* (2006). This allows us to place point magnetic sources on a spherical photosphere and calculate meaningful topological results for the full 3D global coronal magnetic field. A potential magnetic field is used – a reasonable first approximation for the global coronal

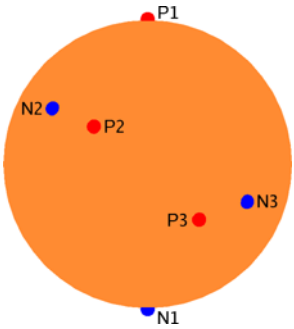

Figure 1 Source setup for the topological field reversal model.

Table 1 Locations and roles of the magnetic point sources in the model.

Source	θ coordinate	φ coordinate	Role in model
P1	0	0	North pole
P2	$\frac{5\pi}{12}$	$\frac{\pi}{8}$	North leading polarity
P3	$\frac{5\pi}{8}$	$\frac{3\pi}{8}$	South following polarity
N1	π	0	South pole
N2	$\frac{3\pi}{8}$	0	North following polarity
N3	$\frac{7\pi}{12}$	$\frac{\pi}{2}$	South leading polarity

field (which is not far from being potential; Pneuman, Hansen, and Hansen, 1978), and one whose results can easily be generalised to apply to more realistic magnetic fields containing stored magnetic energy, *e.g.*, nonlinear force-free fields (Régnier, Amari, and Kersalé, 2002; Mackay and van Ballegooijen, 2006a, 2006b; Schrijver *et al.*, 2006). The model is intended to represent the large-scale global magnetic field in the corona throughout the process of polar field reversal. As such, the potential field approximation is appropriate, because the coronal field is generally close to potential except inside active regions, and only the large-scale field is considered here.

Figure 1 shows the six-source setup used in the model. The dominant dipolar field is represented by a source at each pole, another two represent a large bipolar region of emerging flux in the northern hemisphere, and the final two represent a similar region in the southern hemisphere. The emerging flux regions are placed near the middle of the sunspot bands in each hemisphere. For the exact coordinates chosen, we refer to Table 1. The idea is to capture the topological nature of field reversal in as simple a manner as possible, which may later be refined and improved. For this reason, we have used only a small number of flux sources to represent, at each step in the evolution, the most likely state that the Sun would be in, *i.e.*, with the large-scale field determined by one large active region in each hemisphere as well as the field from the poles, which is the subject of this work. This is not to say that one active region lasts for many years, but it is approximating the field at any one time by just one active region in each hemisphere together with the polar fields, following the same spirit as Zhang and Low (2001, 2002, 2003). Of course, a more sophisticated model would have several active regions at any one time and would also assume their lifetimes were shorter, of order a solar rotation or so.

The idealised evolution takes the model Sun from solar minimum up through the polar field reversal near solar maximum and back down to the next minimum. Figure 2 shows

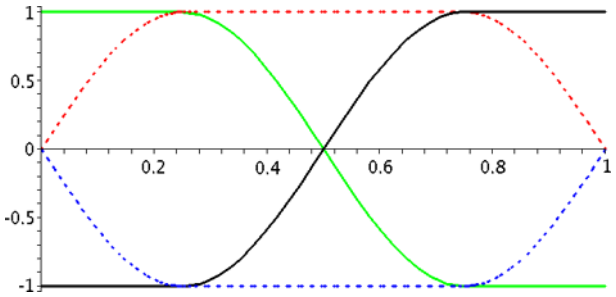

Figure 2 Evolution of magnetic flux in the various sources of the model, shown as the phases of the cycle (x-axis) versus the relative strengths of the sources (y-axis). Green represents the source at the north pole, red the positive active region sources, blue the negative active region sources, and black the source at the south pole.

how the relative strengths of the six flux sources evolve throughout the modelling. At first the dipolar field dominates, so the initial setup has P1 and N1 relatively strong (with strength normalised to ± 1). The newly emerging active regions start off very small, with the sources having relative strengths of ± 0.025. As the cycle begins, the strengths of the active regions are increased, keeping note of all the changes in topology, until their sources have the same strength as the polar sources. This simulates the increased amount of flux emergence that occurs as the cycle progresses. For comparison, a typical polar flux is around 10^{22} Mx (Benevolenskaya, 2004), and a typical large active region flux is about the same. After this, the strengths of the polar sources are gradually decreased until they disappear completely, simulating the cancellation of flux between the poles and the following polarities in the active regions. This stage corresponds to solar maximum, when the dipolar field is no longer dominant, and the large active regions determine the global structure of the coronal magnetic field.

On the Sun, the following polarities of the active regions continue to be preferentially transported towards the poles, so the polar field reverses sign and increases in magnitude. When the polar sources have reached their maximum strength, the active region sources in turn begin their gradual decrease in strength. Solar minimum is reached once more when the strengths of the active region sources become sufficiently low, thus completing one-half of a full 22-year solar cycle. At this stage, the signs of the leading and following polarities of the active regions change, and the process continues with every polarity being opposite to what has just been described. It is clear that no different topological behaviour will be found in the second half of the cycle and so the modelling ends here.

Previous observations of the Sun's magnetic field throughout the cycle (Gibson *et al.*, 1999) have shown that there is often a single "last best active region" that remains in one hemisphere near the end of the cycle when all major magnetic activity has ceased in the other hemisphere. Incorporating this into the next generation of point-source models would be very worthwhile and interesting, as would accounting for features such as the "elephant's trunk coronal hole" also described in that paper.

3. Topological Evolution through the Solar Cycle

3.1. Format of Diagrams and Classification of Topologies

In this section, we present a sequence of diagrams illustrating the coronal magnetic topology at various stages throughout the field reversal process. For each topology, the 3D view of the field lines on the sphere uses the following notation: positive/negative point magnetic flux sources are red/blue spheres, labelled P/N; positive/negative magnetic null points are

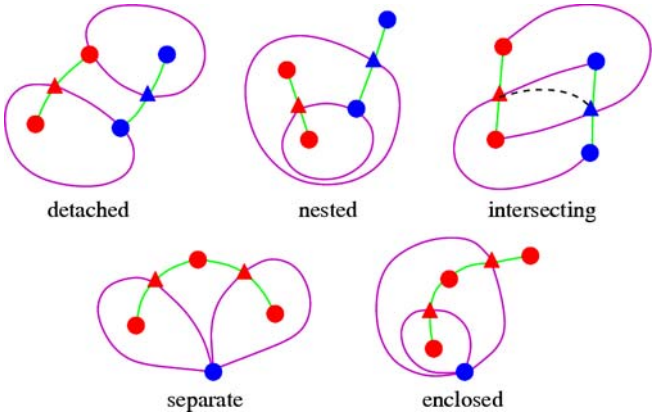

Figure 3 Idealised sketch of the five four-source spherical topologies from Maclean *et al.* (2006) and Maclean, Beveridge, and Priest (2006) used in the present work.

red/blue tetrahedra, labelled B/A; spine fieldlines are green; field lines in separatrix surfaces are purple. For each topology there is also an idealised sketch showing its photospheric footprint and the locations of all the separators; the two sources at the top and bottom are those whose flux forms the dominant flux domain, and the separatrices all close down to form domes as suggested by the directions in which they curve. Separators are indicated by dashed black lines. Finally, the domain and null graphs are presented. The domain graph shows which sources are linked by flux domains, and the null graph shows which nulls are linked by separators.

Maclean *et al.* (2006) and Maclean, Beveridge, and Priest (2006) catalogued all the possible topological states for four magnetic sources on a sphere in a potential field. Their results can be interpreted as providing a method of classifying the relationship of separatrix surfaces with each other. Figure 3 summarises those four-source states that are necessary to our current model; for more detail see Beveridge, Priest, and Brown (2002, 2004). The separatrices of two nulls of the same sign can configure themselves in either a separate state or an enclosed state (there are no upright null states in this model), and two nulls of opposite sign can give rise to a detached, nested, or intersecting state (there are no coronal nulls and, as it turns out, no dual intersecting states in this model). There are two positive and two negative nulls in each topology here, so there are six relationships to consider: that of B1 to B2, B1 to A1, B1 to A2, B2 to A1, B2 to A2, and A1 to A2. From now on, for simplicity, we will say *e.g.*, "A1 and B2 are nested" to mean "the separatrix surfaces of nulls A1 and B2 form a nested state." These states may be exactly as described in Maclean *et al.* (2006), in which case we refer to them as *pure* examples of the state, or they may have the same overall form but include extra spines or separators, in which case they are called *compound*. If the connectivity of one null's spine and separatrix is simple but the other includes extra spines or separators then it is called a *hybrid* state. The differences should become apparent as examples of both are studied in the next section.

Three types of topological bifurcation take place in the model, all of which have been previously studied in the literature. The *global spine-fan bifurcation* (Brown and Priest, 1999b) involves the spine of one null point flipping through the separatrix surface of another like-signed null, creating or destroying flux domains as it goes. The *global separator bifurcation* (Brown and Priest, 1999a) is similar but involves two oppositely signed separatrix surfaces instead of one separatrix and one spine. Finally, the *global separatrix quasi-*

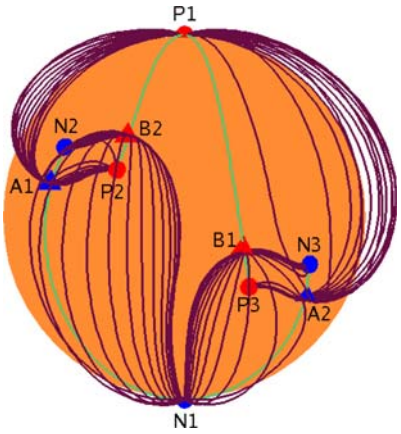

(a) 3D view of the topology on the sphere. Positive/negative point magnetic flux sources are red/blue spheres, labelled P/N; positive/negative magnetic null points are red/blue tetrahedra, labelled B/A; spine field lines are green; field lines in separatrix surfaces are purple.

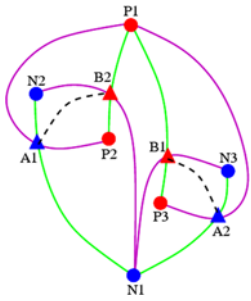

(b) Simplified sketch of photospheric footprint and separators. The two sources at the top and bottom are those whose flux forms the dominant flux domain, and the separatrices all close down to form domes as suggested by the directions in which they curve. Separators are indicated by dashed black lines.

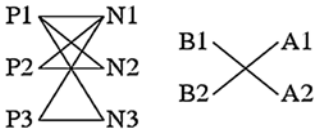

(c) Domain graph (left) and null graph (right). The domain graph shows which sources are linked by flux domains, and the null graph shows which nulls are linked by separators.

Figure 4 The topology when the strength of the active region sources is ± 0.025, before any bifurcations have taken place. The bipolar field from the poles is dominant, and the two active regions are not magnetically linked.

bifurcation (Beveridge, Priest, and Brown, 2002) does not create or destroy flux domains, but rather changes which flux domain is *dominant*, *i.e.*, has field lines that extend out towards infinity (in a topological state with flux balance).

3.2. Waxing Cycle: From Solar Minimum to Maximum

The sequence of topologies begins just after solar minimum with the strong bipolar field from the polar sources dominating the flux from the newly emerging active region bipoles (relative source strength ± 0.025), as shown in Figure 4. The two active regions in the north and south hemispheres are not magnetically connected; instead, each active region forms a *pure intersecting* state along with P1 and N1, giving two separators (B1 – A2 and B2 – A1) in the topology. Both B1 and A1, and B2 and A2, form *compound detached* states, and B1 and B2 are *compound separate*, as are A1 and A2. The number of flux domains and separators present for each topology studied here have all been checked against the Beveridge – Longcope equation (Beveridge and Longcope, 2005) to ensure that no topological features have been overlooked.

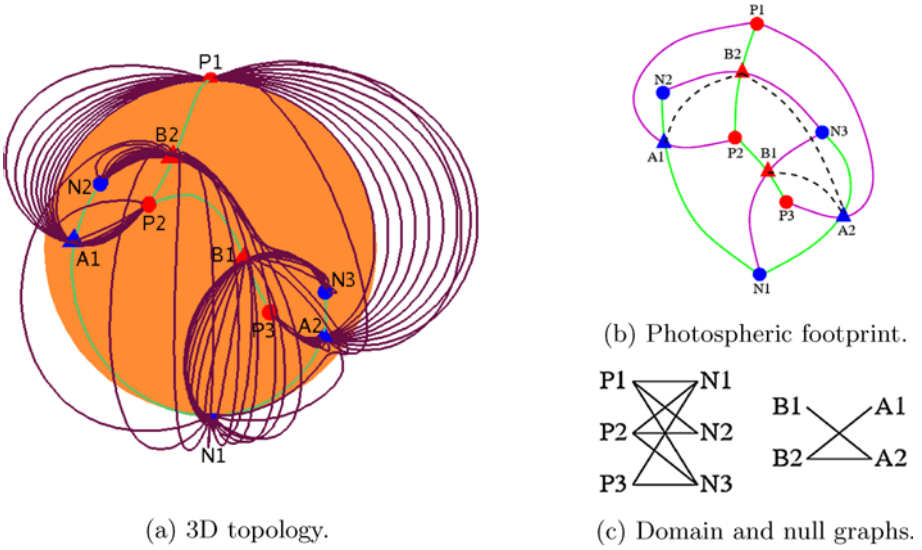

Figure 5 The topology when the strength of the active region sources is ± 0.1, after the global spine-fan bifurcation (β_1) between B1 and B2 that magnetically links the two active regions, forming the first transequatorial loops.

The first change occurs when the strengths of the active region sources are in the range ± 0.05 to ± 0.1. A global spine-fan bifurcation (β_1) between B1 and B2 takes the topology to the configuration seen in Figure 5. Maclean *et al.* (2005) explain why, if $\mathcal{S}'$ is the set of all the separators of the null (S) whose spine is involved in the bifurcation, and $\mathcal{T}'$ is the separator set of the null (T) whose separatrix is involved in the bifurcation, the global spine-fan bifurcation changes the separators in the topology such that, afterwards, the set of separators connected to null T is everything that was connected to T, but not S before, plus everything that was connected to S, but not T before. In set notation, the set of separators connected to null T after the bifurcation is $\mathcal{U}' = \{\mathcal{T}' \backslash \mathcal{S}'\} \cup \{\mathcal{S}' \backslash \mathcal{T}'\}$. Null S does not change its separators.

In this case, S is B1 and T is B2, so $\mathcal{S}'$ is {A2} and $\mathcal{T}'$ is {A1}. This means that $\mathcal{U}'$ is {A1, A2}. So after the bifurcation, B1 is still connected to A2, and B2 connects to both A1 and A2, as is confirmed by the null graph. The creation of the third separator means that there are now two *hybrid* (B1 and A2; B2 and A1) and one *compound* (B2 and A2) *intersecting* states. Note that this means the global spine-fan bifurcation can change one variety of intersecting state to another. This was not discovered by Maclean *et al.* (2006) because, with only four sources, it is impossible for a global spine-fan bifurcation to occur in a topology containing an intersecting state. B1 and A1 are still *compound detached*.

However, from Maclean, Beveridge, and Priest (2006), the global spine-fan bifurcation can change separate states to enclosed states. Thus it makes sense that for the like-signed nulls, although A1 and A2 are still *compound separate*, B1 and B2 are now *compound enclosed*.

The physical significance of this topology is that the two active regions have formed a magnetic connection across the equator, so we predict that transequatorial loops will begin forming at around these parameter values. The field from the poles still completely dominates the topology.

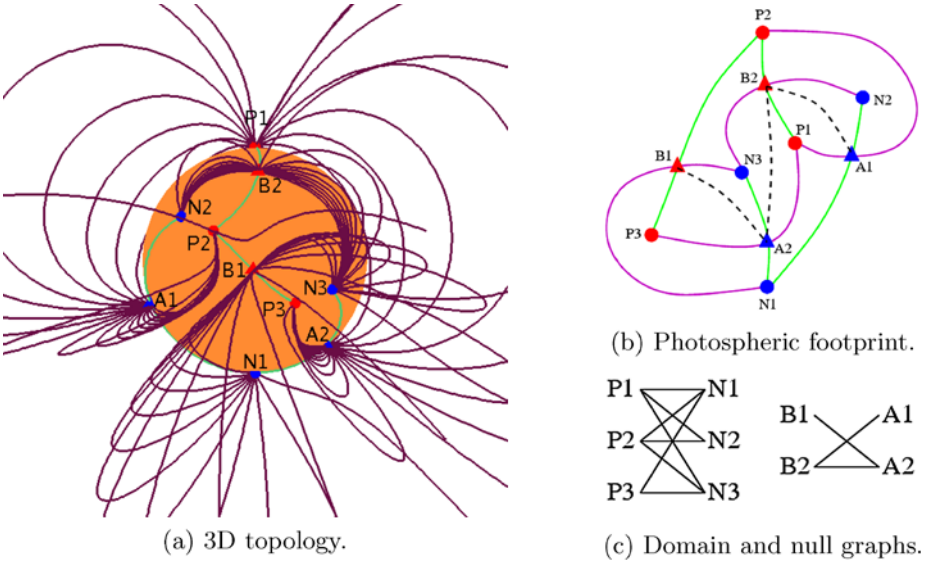

Figure 6 The topology when the strength of the active region sources has peaked at ± 1 and that of the polar sources has decreased to ± 0.5. The bipolar field has begun to lose its dominance as B2 has undergone a global separatrix quasi-bifurcation (β_2) leaving the dominant flux domain as P2 – N1.

There is a long gap before the next bifurcation, a global separatrix quasi-bifurcation (β_2), which does not occur until after the strengths of the active region sources have increased to their maximum of ± 1 and the polar sources have decreased to somewhere between ± 1 and ± 0.5. Figure 6 shows the new topology. The separatrix of B2 has expanded out to infinity and contracted back down to cover a different set of sources (specifically, P1 instead of P2 and P3). The effect of this is to make B1 and B2 *compound separate* instead of compound enclosed, as is allowed by the results of Maclean, Beveridge, and Priest (2006). All other relationships between the nulls are unchanged.

Physically, the global separatrix quasi-bifurcation represents a change in which two flux sources dominate the topology. In this case, P1 at the north pole loses its dominance as the field begins its reversal process, and the new dominant flux domain is P2 – N1. P2 is the leading polarity of the northern hemisphere active region, and it is natural that it should take over dominance as P1 weakens, because it is the closer of the two other positive sources to P1.

Figure 7 shows the next topology in the sequence. Two more bifurcations have occurred to reach this state, both when the polar source strengths are between ± 0.5 and ± 0.25. In fact, the two bifurcations are closely linked. As the polar flux continues to weaken, B1 undergoes a global separatrix quasi-bifurcation (β_3) that makes P3 – N1 the dominant flux domain. Its separatrix folds down round the back of the sphere and as it does so, it undergoes a global separator bifurcation (β_4) with A1.

The global separatrix quasi-bifurcation causes B1 to cover B2 in a *compound enclosed* state. A1 and A2 are still *compound separate*. As for the oppositely signed nulls, the global separator bifurcation creates a fourth separator (B1 – A1), meaning that there are four *compound intersecting* states in the topology. The effect of the global separator bifurcation in creating this last separator is to complete the process of connecting the active region bipoles;

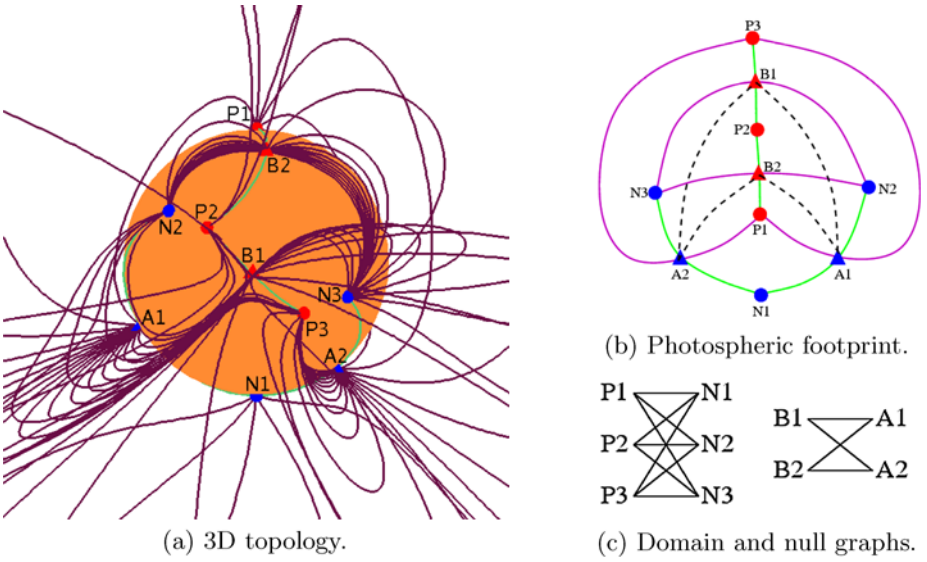

(a) 3D topology. (b) Photospheric footprint. (c) Domain and null graphs.

Figure 7 The topology when the strength of the polar sources is ± 0.25. The dominant flux domain has changed again, to P3 – N1, via a global separatrix quasi-bifurcation (β_3) of B1. This in turn leads to A1 and B1 undergoing a global separator bifurcation (β_4), which completes the connection between the two active region bipoles.

now each of the four sources is magnetically connected to all the others. So at these parameter values, the observed transequatorial loops should be fully formed and bright.

Another global separatrix quasi-bifurcation (β_5) then occurs when the polar source strengths are between ± 0.25 and ± 0.1. The new topology is shown in Figure 8. This time it is A2 whose separatrix is involved; it switches from covering N3 to covering N1 and N2, leaving P3 – N3 as the dominant flux domain. So at this stage, the original bipolar field is no longer significant, and flux from the active region bipole in the southern hemisphere dominates the system. With regard to the separatrices, the global separatrix quasi-bifurcation leaves A2 covering A1 in a *compound enclosed* state, and the other relationships do not change.

The fact that the original bipolar field no longer dominates the magnetic structure of the system may have an effect on the frequency of CMEs leaving the corona. Throughout most of the solar cycle, there is a strong bipolar component to the overlying magnetic field, coming from the poles, but near solar maximum this component becomes very weak or even disappears altogether. When this happens, it should be easier for any potential CME to lift off, because there is less overlying field holding it down; less reconnection needs to occur for the CME to escape. So in this model, it is not solely the number of potential CME-producing ARs that predicts how many CMEs will occur; the topological state of the overlying magnetic field also plays a role.

A significant development occurs when the strengths of the polar sources are between ± 0.1 and ± 0.05. As shown in Figure 9, the negative source at the south pole becomes topologically isolated, with all of its flux contained inside one unbroken separatrix dome. This happens via a global spine-fan bifurcation (β_6) involving the spine of A1 and the separatrix of A2. In terms of the analysis mentioned previously, A1 is S and A2 is T, so $\mathcal{S}'$ is $\{\mathrm{B1}, \mathrm{B2}\}$ and $\mathcal{T}'$ is also $\{\mathrm{B1}, \mathrm{B2}\}$. Hence $\mathcal{U}'$ (every null previously connected to T but not S by separators, and every null previously connected to S but not T) is the empty set, and so after

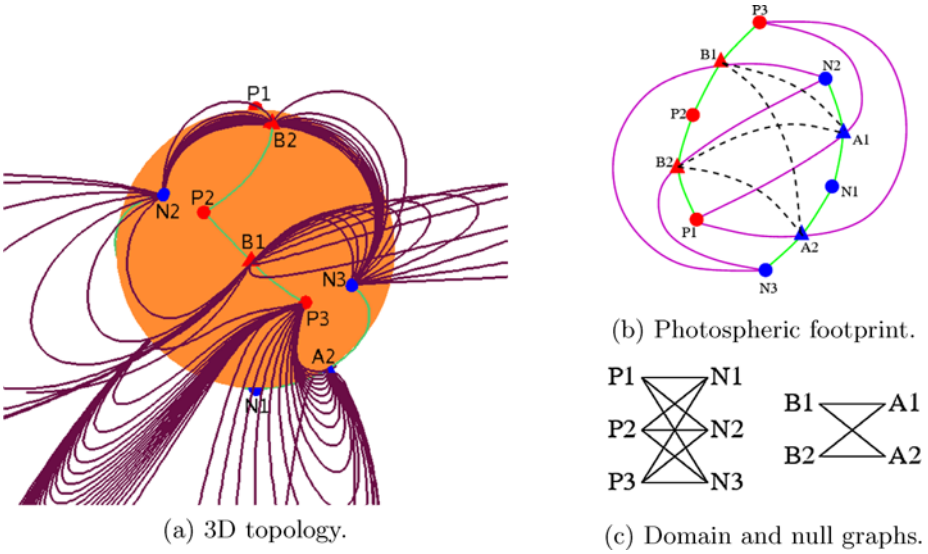

Figure 8 The topology when the strength of the polar sources is ± 0.1, after another global separatrix quasi-bifurcation (β_5; this time of A2) that changes the dominant flux domain to P3 – N3, ending completely the influence of the polar field.

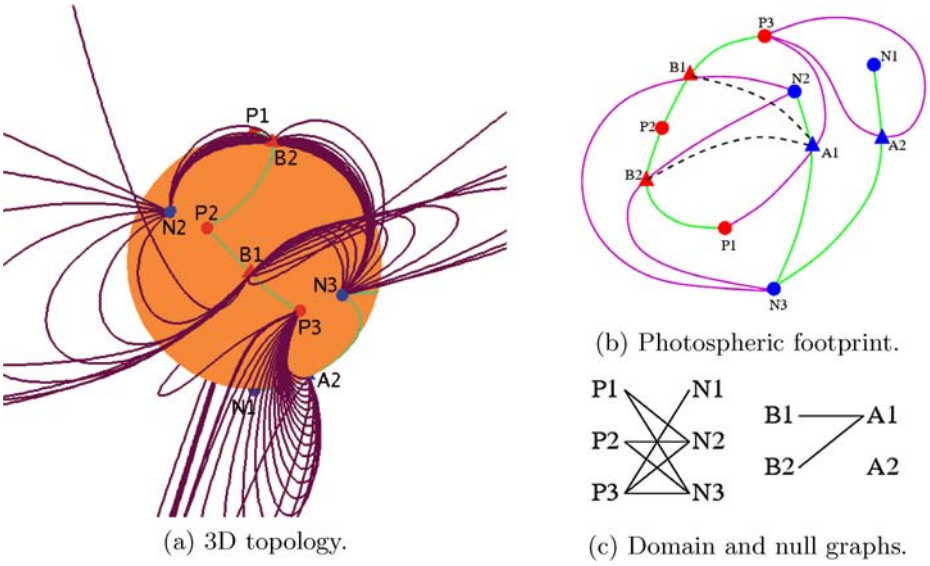

Figure 9 The topology when the strength of the polar sources is ± 0.05, after a global spine-fan bifurcation (β_6) involving A1 and A2 has isolated the flux from N1 in a single flux domain.

the bifurcation A1 is still connected to B1 and B2, but A2 has lost both of its separators and forms a simple dome.

The disappearance of the two separators means that only two *hybrid intersecting* states remain, which are formed by B1 and A1 and by B2 and A1. It is interesting to notice from

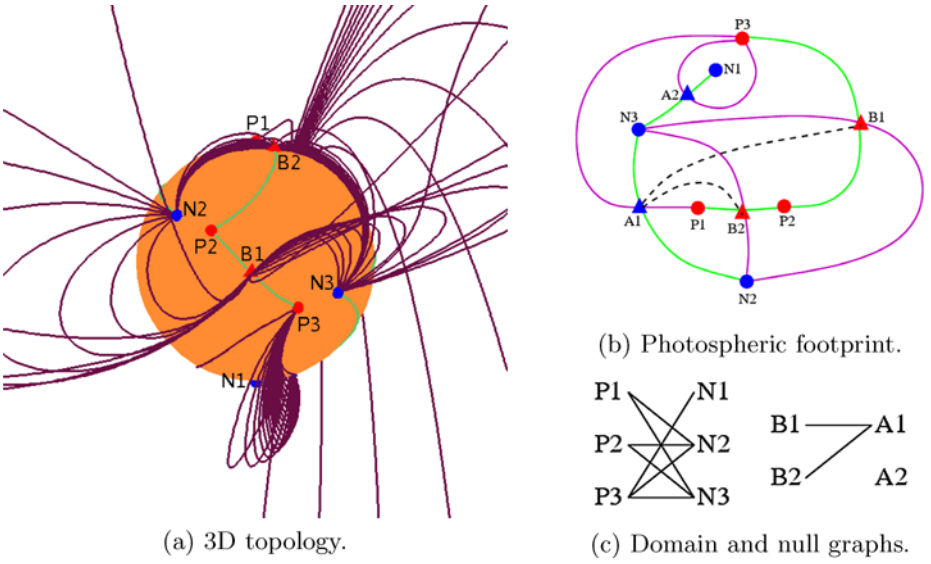

Figure 10 The topology when the strength of the polar sources is ± 0.025, after a global separatrix quasi-bifurcation (β_7) of A1 that completes the transfer of the dominant role in terms of flux to the following polarities of the active regions, so that P3 – N2 is the dominant flux domain.

this example that the global spine-fan bifurcation can turn intersecting states into *detached* ones, here producing such (*hybrid*) states between B1 and A2 and between B2 and A2. This was not observed by Maclean *et al.* (2006) as with only four flux sources it is not possible to find global spine-fan bifurcations occurring in a topology containing intersecting or detached states.

It is known, however, that global spine-fan bifurcations can turn enclosed states into separate ones, and this happens here with A1 and A2 forming a *hybrid separate* state. B1 and B2 are still *compound enclosed*.

Physically, the weakness and magnetic isolation of the field of the south pole can be interpreted to mean that the south polar coronal hole has disappeared, as does indeed happen in the approach to solar maximum (Harvey and Recely, 2002). Field lines from the polar region are all now closed, no longer reaching high in to the solar atmosphere to dominate the corona, so coronal-hole-type structures are impossible at these parameter values.

The next bifurcation is a global separatrix quasi-bifurcation (β_7) of A1, its separatrix moving round the back of the sphere to cover N1 and N3 instead of N2, as seen in Figure 10. The bifurcation occurs when the strengths of the polar sources are between ± 0.05 and ± 0.025. The separatrix of A1 now covers that of A2 in a *hybrid enclosed* state. This makes the dominant flux domain P3 – N2, and so it remains until after the polar fields have reversed in sign. Thus the field of the following polarities of the active regions is dominant during the field reversal process. It is the following polarities rather than the leading ones that take this role because of Joy's law; the axis tilt of the bipoles means that the flux from the leading polarities mostly cancels low in the corona over the equator, leaving the following polarity flux to dominate.

The last true bifurcation of the waxing solar cycle occurs when the strengths of the polar sources have been reduced to between ± 0.01 and ± 0.001. It is a global separator bifurcation (β_8) involving B2 and A1, and it has the effect of both destroying a separator and isolating

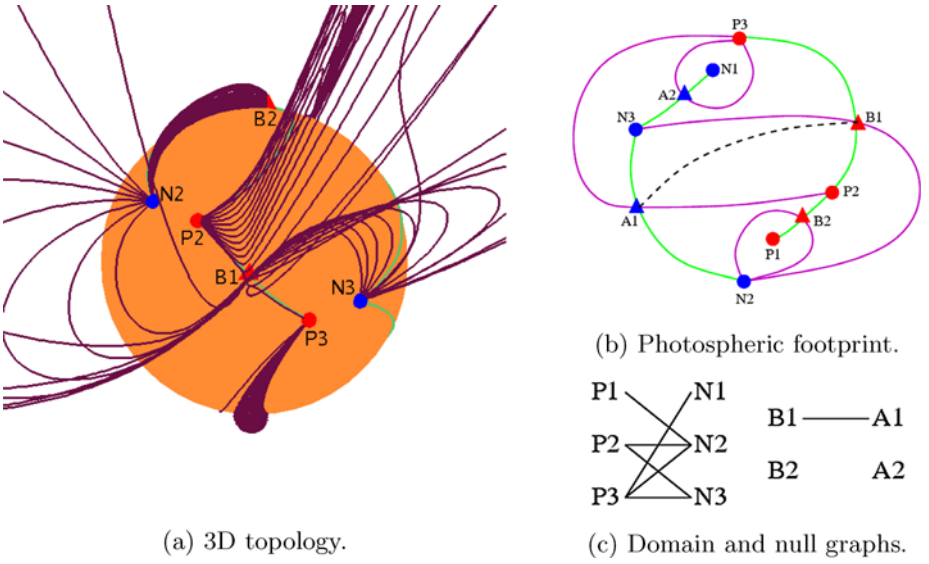

Figure 11 The topology when the strength of the polar sources is ± 0.001, after a global separator bifurcation (β_8) between B2 and A1 that isolates the flux of P1 in a single domain.

P1, the source at the north pole, under a single unbroken separatrix surface, as can be seen in Figure 11. Physically, this corresponds to the loss of the north polar coronal hole. Maclean *et al.* (2006) showed that the global separator bifurcation can change intersecting states to detached states, and this is what happens here with the loss of the separator and the creation of the *hybrid detached* state associated with B2 and A1.

The change in position of the separatrices causes the B1 – A1 intersecting state to alter its nature and become a *pure intersecting* state. Clearly, also, the enclosed states from both A1 and A2, and B1 and B2, are now *hybrid* in nature. Just as with the global spine-fan bifurcation previously, this shows that global separator bifurcations can change a topology from one version of an enclosed state to a different one. This was not discovered in the four-source case because of the impossibility (in that case) of a global separator bifurcation occurring in an enclosed configuration.

When the strengths of the sources at the poles pass through zero as they reverse sign, there is an isolated state in which only the four active region sources are present. Although it is not a true bifurcation as it involves disappearance of sources, it is a change in the magnetic topology, and we will therefore call it β_9. As P1 and N1 disappear, they take with them the nulls whose separatrices contain their flux, and they leave only a *pure intersecting* state, as shown in Figure 12. The flux from the following polarities still dominates the high corona. It is unlikely that a state such as this could occur in practice because the reversal is normally not entirely symmetric (*i.e.*, the field at one pole usually reverses sign a few months before the other one). However, the states directly before and after this one show that when the polar fields are very small they are effectively isolated, and the following polarities of the active regions dominate. This is another prediction from the model that could be tested against the observations: that most of the open magnetic flux should originate in the active regions near solar maximum.

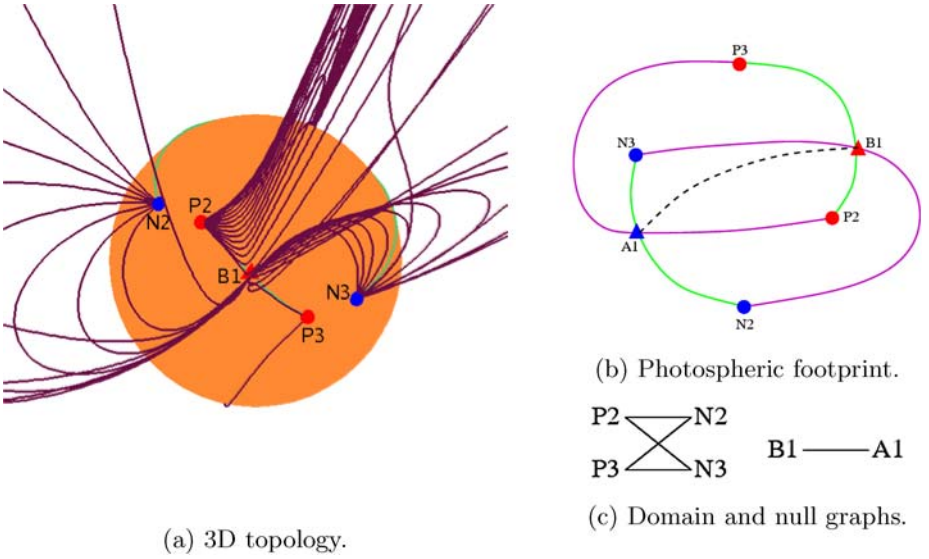

Figure 12 The topology at the point of field reversal (β_9), *i.e.*, only the four active region sources remain. The topological structure is that of the intersecting state from Maclean *et al.* (2006).

This topology marks the theoretical maximum of the solar cycle, the moment of reversal of the polar fields. In the next section, oppositely signed polar sources are reintroduced, and the topological states and bifurcations involved in the waning part of the cycle are discussed.

3.3. Waning Cycle: From Solar Maximum Back to Minimum

The new polar sources (which are still called P1 and N1 but have swapped positions with each other) are given an initial strength of ± 0.001, which is below the level at which the first bifurcation occurs. In this initial state (β_{10}), just after solar maximum, the polar sources are isolated from the rest of the topology, each lying under its own unbroken separatrix surface. The separatrices belong to the two new nulls that have also appeared, still called B2 and A2. All this can be seen in Figure 13.

Since the separatrices of B2 and A2 are unbroken, and both are covered by the separatrices of nulls of the opposite sign, there are two *hybrid nested* states, associated with B1 and A2 and with B2 and A1. The *pure intersecting* state (A1 and B1) survives from the previous topology. And the last oppositely signed null combination, B2 and A2, of course forms a *compound detached* state. B1 and B2, just like A1 and A2, are *hybrid separate*.

The first bifurcation in this second half of the cycle is a global spine-fan bifurcation (β_{11}), taking place when the strength of the polar sources has just begun to increase and is between ± 0.001 and ± 0.00175. Figure 14 shows the resulting topology. A1 is the S null and A2 is the T null, so that $\mathcal{S}'$ is {B1} and $\mathcal{T}'$ is the empty set. This gives $\mathcal{U}'$ as {B1}, so that after the bifurcation A1 still has a separator to B1, and a new separator B1 – A2 is created.

The global spine-fan bifurcation has several effects in this instance: it changes the B2 – A2 compound detached state to a *hybrid nested* state, the B1 – A2 hybrid nested state to a *hybrid intersecting* state, the B1 – A1 pure intersecting state to a *hybrid* version, and the A1 – A2 hybrid separate state to a *compound enclosed* state. This topology is unusual in being "double nested" – three of its separatrix domes stack inside each other like Russian dolls.

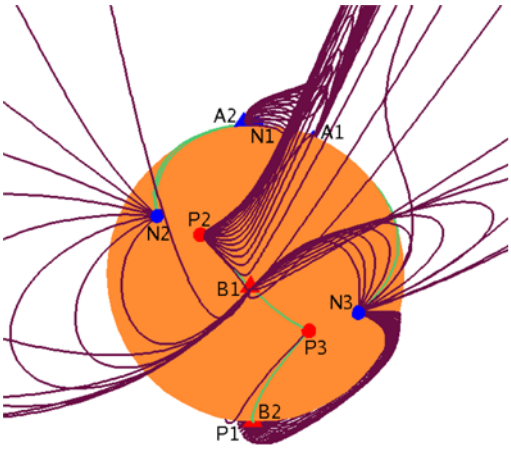

(a) 3D topology.

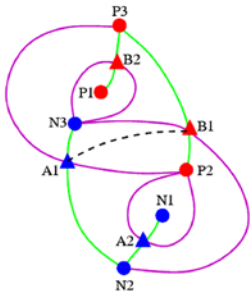

(b) Photospheric footprint.

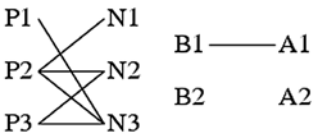

(c) Domain and null graphs.

Figure 13 The topology when the strength of the newly emerging polar sources is ± 0.001 (β_{10}). The new poles are topologically isolated, with all their flux confined in one simple domain each. P3 – N2 is still the dominant flux domain.

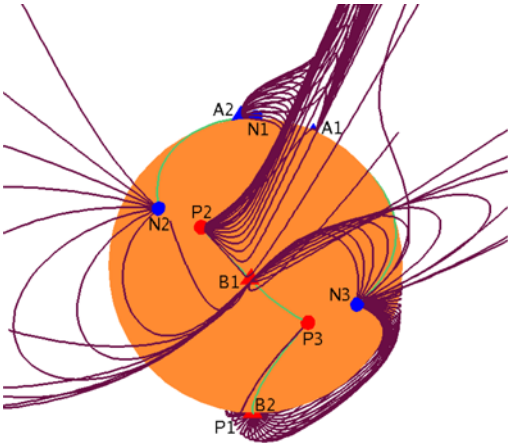

(a) 3D topology.

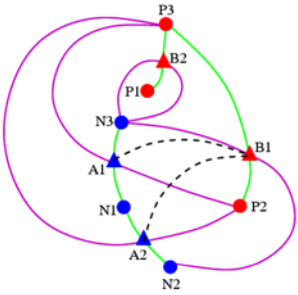

(b) Photospheric footprint.

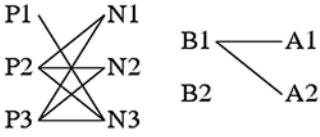

(c) Domain and null graphs.

Figure 14 The topology when the strength of the polar sources is ± 0.00175, after a global spine-fan bifurcation (β_{11}) between A1 and A2 has allowed N1 to connect back into the topology.

Physically, this bifurcation represents the flux of the new northern polar source, N1, connecting back in to the topology from its previously isolated state, and hence the reappearance of the northern polar coronal hole.

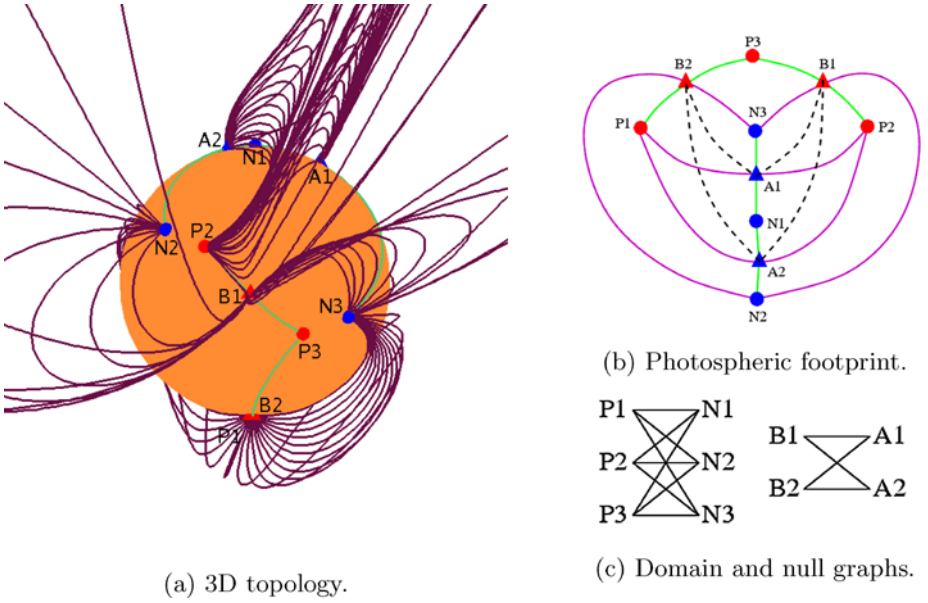

(a) 3D topology.

(b) Photospheric footprint.

(c) Domain and null graphs.

Figure 15 The topology when the strength of the polar sources is ±0.01, after a sequence of two global separator bifurcations (β_{12} and β_{13}) has allowed P1 to connect back into the topology. First B2 and A1, and then immediately B2 and A2, undergo this bifurcation.

The next two bifurcations take place as the strengths of the polar sources continue to increase, to somewhere between ±0.0025 and ±0.005. Both are global separator bifurcations (β_{12} and β_{13}), one between B2 and A1, and the other between B2 and A2. The result can be seen in Figure 15. A physical interpretation is that the increasing flux from P1 can no longer be balanced solely by flux from N3, and so the separatrix of B2 needs to expand. It does this through the global separator bifurcations, creating two new separators along the way and turning both the nested states into *compound intersecting* ones. The creation of the new flux domains from P1 to the other negative sources corresponds to the reappearance of the southern polar coronal hole.

Another effect of the global separator bifurcations is to change the nature of the *compound enclosed* state of A1 and A2; now both separatrices run along both positive spines instead of just one. In addition, B1 and B2 now form a *compound separate* state, showing that the global separator bifurcation can change one variety of separate state to another.

When the strengths of the polar sources have increased to between ±0.05 and ±0.1, null A2 undergoes a global separatrix quasi-bifurcation (β_{14}). This switches the dominant flux domain to P3 – N1, so that the polar field begins to reassert its dominance, as can be seen in Figure 16. The effect of the bifurcation is to switch the compound enclosed state of A1 and A2 to being *compound separate*. The topology now is very symmetrical, with four compound intersecting states and two compound separate states. Interestingly, this is the only topology of all those studied here that is truly spherical in the sense that it cannot be drawn in the plane without distortion. In Figure 16b, the two negative separatrices close down outwards round the back of the sphere, as indicated by the arrows.

Another global separatrix quasi-bifurcation (β_{15}) then takes place when the strength of the polar sources is between ±0.25 and ±0.5. This time it is the separatrix of B2 that flips over, to cover P2 and P3 instead of P1. The dominant flux domain is now P1 – N1, so the

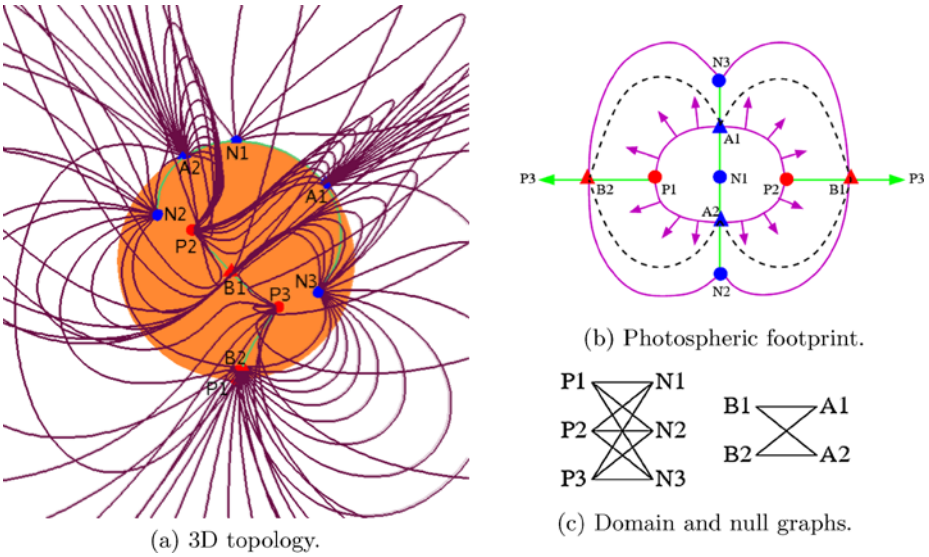

Figure 16 The topology when the strength of the polar sources is ± 0.25, after the first global separatrix quasi-bifurcation (β_{14}) of the waning cycle. The separatrix of A2 flips over, leaving P3 – N1 as the dominant flux domain. The growing polar flux has begun to assert its influence. Note that the topology shown here is truly spherical and cannot be properly sketched flat. In (b), separatrices with arrows close outwards along the positive spine line that passes through P3 on the other side of the sphere.

polar flux has reconquered the corona and will not be overcome again during this cycle. In terms of observables, the fact that the bipolar field dominates the corona again means that the rate of CMEs should fall as the strong overlying field is back in place.

The bifurcation changes the compound separate state of B1 and B2 to a *compound enclosed* state. In fact, this topology has the same essential structure as the previous topologies in Figures 8 and 15, allowing for relabelling of sources and nulls. At first sight it seems surprising that the same topology recurs so often in a system as complex as this, but in fact there are only three possible basic topologies in which all four nulls are joined by separators: both pairs of like-signed nulls in a separate configuration, both in an enclosed configuration, or one pair separate and one enclosed. Remember that this does not take into account relabelling of sources (*i.e.*, which flux domain is dominant), which can hugely increase the number of possible variants of each of the three basic states just mentioned. The previous topology (see Figure 16) is an example with both like-signed null pairs in a separate configuration, and the topology in Figure 8 is an example with both like-signed null pairs in an enclosed state.

With the next bifurcation, it is becoming obvious that the topology is settling back towards a solar-minimum-type state, as shown in Figure 18. The active region bipoles, which have been fully connected to each other since the third bifurcation of the waxing cycle, begin to disconnect via a global separator bifurcation (β_{16}) once the strengths of the active region sources start to decrease, reaching between ± 1 and ± 0.5. This means that the transequatorial loops will begin to disappear. The separatrices of B1 and A1 lose their intersection (and therefore their separator), moving to a *compound detached* state. The intersecting states of B1 and A2, and of B2 and A1, also change their nature from compound to *hybrid intersecting*. Subject to relabelling, this is the same topological structure seen near the beginning of the waxing cycle in Figure 5.

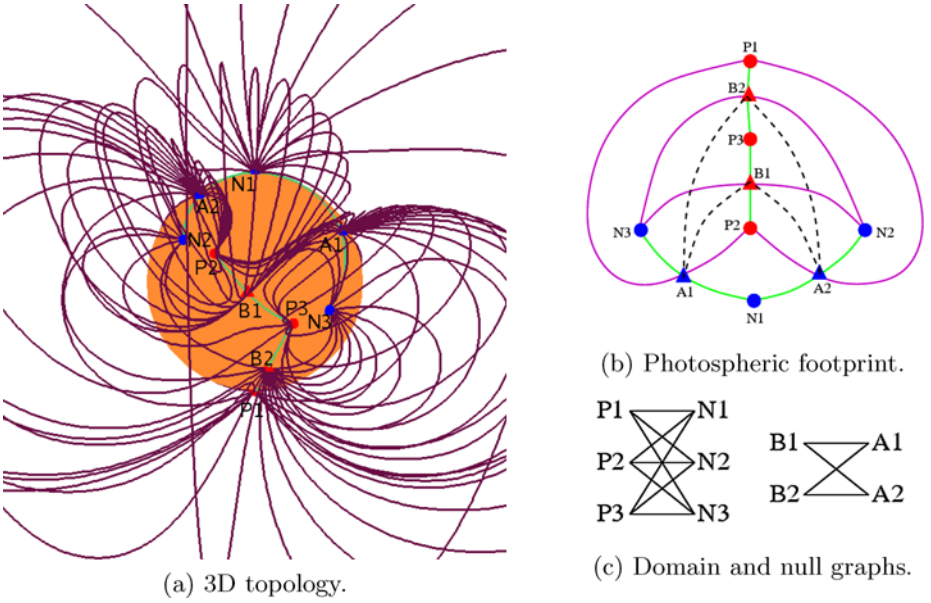

Figure 17 The topology when the strength of the polar sources is ± 1, equalling that of the active region sources. Another global separatrix quasi-bifurcation (β_{15}), this time of B2, allows the polar field to regain its dominance, so that P1 – N1 is again the dominant flux domain.

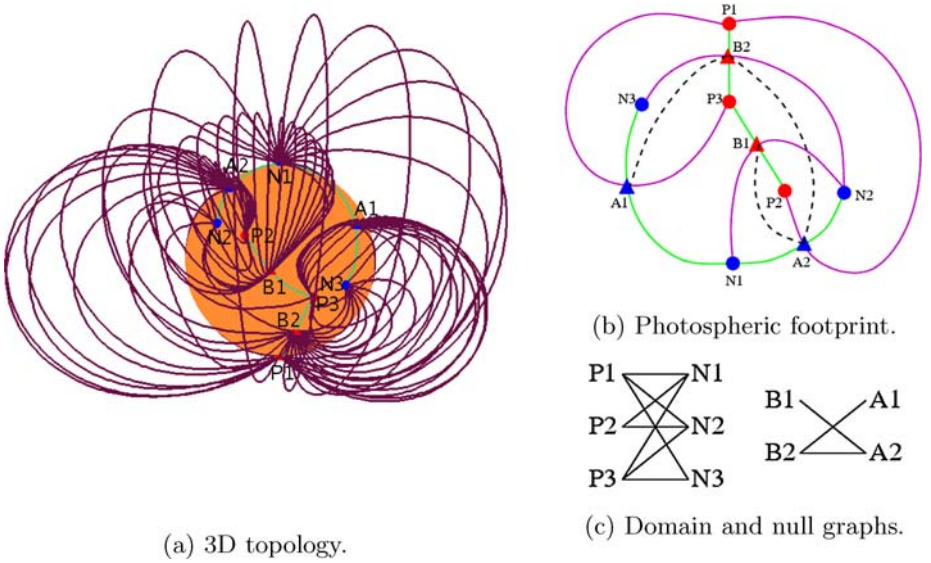

Figure 18 The topology when the strength of the active region sources is ± 0.5, when a global separator bifurcation (β_{16}) between B1 and A1 has started the process of disconnecting the active region bipoles from each other. They are now only linked by one separator.

The final bifurcation occurs when the strengths of the active region sources have decreased further, to between ± 0.25 and ± 0.1. The active region bipoles disconnect entirely in

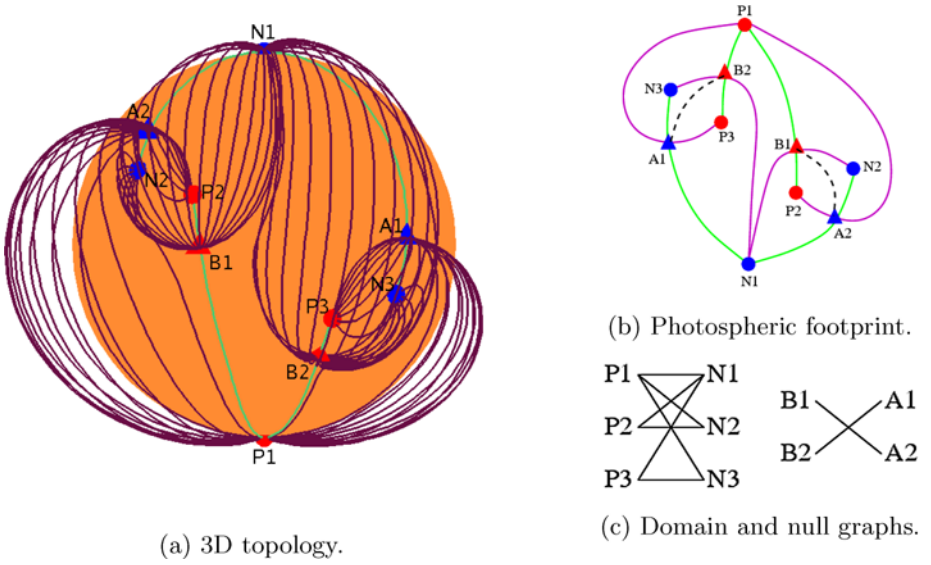

Figure 19 The final topology, when the strength of the active region sources is ± 0.05. The active region flux is rapidly decreasing. The bipolar field from the poles is dominant, and the two active regions are no longer magnetically linked after the global spine-fan bifurcation (β_{17}) that splits them apart. Eventually the active regions will disappear altogether and the field will be purely bipolar.

a global spine-fan bifurcation (β_{17}) between B1 and B2, severing the last remaining transequatorial loops. Figure 19 shows the resulting magnetic topology. In this case, the spine of B1 moves through the separatrix of B2, so B1 is the S null and B2 is the T null, making $\mathcal{S}' = \{\text{A2}\}$ and $\mathcal{T}' = \{\text{A1}, \text{A2}\}$. Hence $\mathcal{U}'$ is $\{\text{A1}\}$, and so after the bifurcation B1 still connects to A2 but B2 has lost its separator to A2, only keeping its connection to A1.

The loss of the separator means that the global spine-fan bifurcation has turned the compound intersecting state between B2 and A2 into a *compound detached* one. It has also changed the relationship of B1 and B2 to *compound separate* from compound enclosed. Lastly, the intersecting states between B1 and A2 and between B2 and A1 have become *pure* in nature. Subject to relabelling, this is the same topological structure seen at the start of the waxing cycle in Figure 4; the cycle has come full circle. Solar minimum will theoretically be achieved when the strengths of the active region sources reach precisely zero and only the bipolar field from P1 and N1 remains. After this, the active regions will begin to reemerge with the opposite source signs, and the process of field reversal will be set in motion all over again.

4. Discussion

In this paper, we have used magnetic charge topology modelling techniques to analyse the polarity reversal of the global solar coronal magnetic field that takes place as a consequence of the 22-year sunspot cycle. Using six magnetic point sources to represent the bipolar field from the polar regions and a large active region in each hemisphere, we varied the strengths of the sources to mimic the variations in the amount of flux present throughout the cycle.

We found that the global magnetic field passes through several distinct stages during the reversal process. Many of these topological structures of the magnetic field correspond to

observable features or changes in the corona, as summarised in Table 2. The starting field at solar minimum is essentially bipolar. First the active regions in different hemispheres connect to each other over the equator. As the flux from the poles becomes weaker, first the leading polarities and then the following polarities of the active regions dominate the topology. Eventually all the polar flux is isolated from the rest of the flux, inside a single simple flux domain at each pole. Then the polar sources reverse sign at solar maximum and begin to increase in magnitude again. At first they are weak and their flux is isolated, but it soon connects back in to the main topology. As the polar flux continues to strengthen it regains its dominance of the coronal magnetic field. The active regions lose their influence and disconnect from each other. At solar minimum the field is once again essentially bipolar in nature.

The model makes several predictions regarding the epochs of the solar cycle at which various observable features should be found. In particular, it has implications concerning the appearance and disappearance of transequatorial loops, the frequency of CMEs near solar maximum, and the disappearance and subsequent reappearance of polar coronal holes.

The results of Maclean *et al.* (2006) and Maclean, Beveridge, and Priest (2006) on four-source topologies were applied to the reversal model and we found that each stage could be described by using the terminology from those papers. Every topology in the reversal sequence features two magnetic null points of each sign, and the relationship between each pair of associated separatrix surfaces could be classified as a four-source topology. In addition, these topologies were subdivided into *pure* examples (those with all spines and separatrices exactly as described in the four-source case) *compound* examples (those with spines and separatrices arranged in the same basic structure but including additional topological features not present in the four-source case), and *hybrid* examples (a combination consisting of one null point with pure features and one with compound features).

The bifurcations studied by Maclean *et al.* (2006) and Maclean, Beveridge, and Priest (2006) also turned out to be capable of making more types of change to the topologies than were noted in those papers. The global spine-fan bifurcation can change intersecting states to detached states and vice versa, intersecting states to other forms of intersecting state, and enclosed states to other forms of enclosed state. And the global separator bifurcation can change intersecting states, detached states, separate states, and enclosed states to other forms of themselves. This information will be very helpful in the analysis of more complex topological systems.

We hope that the results of this simple but revealing model provide a useful alternative perspective on global magnetic field reversal and will pave the way to increasing our understanding of this fascinating phenomenon. Although the field distributions generated by multipolar expansion models may be more realistic, magnetic topology models provide a relatively easy and clear-cut method for understanding the field topology, which is a valuable exercise as it allows us to analyse quantitatively the large-scale structure of the magnetic field. This point-source model is intended as a first-order approximation to the real solar field, a sequence of topologies describing the structure of the large-scale field at any given stage in the sunspot cycle. Within the constraints of the model we have situated the sources as realistically as possible, at the poles and in the centre of the sunspot belt latitudes, but as a next step the model could take account of the dispersal of flux as meridional circulation and differential rotation stretch the flux out towards the polar regions. It could also include the observed fact that flux emergence is not symmetrical in both hemispheres, but typically a "last best" active region persists in one hemisphere near the end of each cycle. This break in symmetry could have important consequences for the global topology at the beginning of the next cycle, leading to an influence of one cycle on the next that is not considered in the current work.

Table 2 Summary of topological changes occurring in the model and their observable consequences where applicable. GSFB = global spine-fan bifurcation; GSB = global separator bifurcation; GSQB = global separatrix quasi-bifurcation.

Bifurcation	Polar/AR $\|\mathbf{B}\|$ ratio	Physical effects	Observable consequences
β_1 (GSFB)	10 – 20	First cross-equator magnetic connections form	Transequatorial loops begin to appear
β_2 (GSQB)	0.5 – 1	N pole loses flux dominance to leading AR source	
β_3 (GSQB) and β_4 (GSB)	0.25 – 0.5	AR connections strengthen; following AR source dominates positive flux	Transequatorial loops more prominent
β_5 (GSQB)	0.1 – 0.25	S pole loses flux dominance to leading AR source	CME frequency increases
β_6 (GSFB)	0.05 – 0.1	S pole topologically isolated	S polar coronal hole disappears
β_7 (GSQB)	0.025 – 0.05	Following AR source dominates negative flux	
β_8 (GSB)	0.001 – 0.01	N pole topologically isolated	N polar coronal hole disappears
β_9	0	Moment of reversal; only AR sources present	Most open field lines originate in ARs
β_{10}	0.001	Polar sources reappear; still isolated	
β_{11} (GSFB)	0.001 – 0.00175	New N pole connects back in	N polar coronal hole reappears
β_{12} and β_{13} (2 GSBs)	0.0025 – 0.005	Dipolar field reestablished but not dominant	S polar coronal hole reappears
β_{14} (GSQB)	0.05 – 0.1	N pole regains flux dominance	
β_{15} (GSQB)	0.25 – 0.5	Dipolar field dominates topology	CME frequency decreases
β_{16} (GSB)	1 – 2	ARs begin to disconnect	Transequatorial loops disappearing
β_{17} (GSFB)	4 – 10	Total disconnection of ARs	Transequatorial loops gone altogether

References

Babcock, H.W.: 1961, *Astrophys. J.* **133**, 572.
Benevolenskaya, E.E.: 2004, *Astron. Astrophys.* **428**, L5.
Beveridge, C., Longcope, D.W.: 2005, *Solar Phys.* **227**, 193.
Beveridge, C., Priest, E.R., Brown, D.S.: 2002, *Solar Phys.* **209**, 333.
Beveridge, C., Priest, E.R., Brown, D.S.: 2004, *Geophys. Astrophys. Fluid Dyn.* **98**, 429.
Brown, D.S., Priest, E.R.: 1999a, *Solar Phys.* **190**, 25.
Brown, D.S., Priest, E.R.: 1999b, *Proc. Roy. Soc. Lond. Ser. A* **455**, 3931.
Brown, D.S., Priest, E.R.: 2001, *Astron. Astrophys.* **367**, 339.
Gibson, S.E., Biesecker, D., Guhathakurta, M., Hoeksema, J.T., Lazarus, A.J., Linker, J., Mikic, Z., Pisanko, Y., Riley, P., Steinberg, J., Strachan, L., Szabo, A., Thompson, B.J., Zhao, X.P.: 1999, *Astrophys. J.* **520**, 871.
Harvey, K.L., Recely, F.: 2002, *Solar Phys.* **211**, 31.
Hornig, G., Priest, E.R.: 2003, *Phys. Plasmas* **10**(7), 2712.
Leighton, R.B.: 1969, *Astrophys. J.* **156**, 1.
Longcope, D.W.: 2005, *Living Rev. Solar Phys.* **2**, 7.
Mackay, D.H., Priest, E.R., Lockwood, M.: 2002, *Solar Phys.* **207**, 291.
Mackay, D.H., van Ballegooijen, A.A.: 2006a, *Astrophys. J.* **641**, 577.
Mackay, D.H., van Ballegooijen, A.A.: 2006b, *Astrophys. J.* **642**, 1193.
Maclean, R.C., Beveridge, C., Priest, E.R.: 2006, *Solar Phys.* **238**, 13.
Maclean, R.C., Beveridge, C., Longcope, D.W., Brown, D.S., Priest, E.R.: 2005, *Proc. Roy. Soc. Lond. Ser. A* **461**, 2099.
Maclean, R.C., Beveridge, C., Hornig, G., Priest, E.R.: 2006, *Solar Phys.* **235**, 259.
Martinez Pillet, V., Sainz Dalda, A., van Driel-Gesztelyi, L.: 2004, In: *35th COSPAR Scientific Assembly*, 1133.
Pneuman, G.W., Hansen, S.F., Hansen, R.T.: 1978, *Solar Phys.* **59**, 313.
Pontin, D.I., Hornig, G., Priest, E.R.: 2005, *Geophys. Astrophys. Fluid Dyn.* **99**, 77.
Priest, E.R., Longcope, D.W., Heyvaerts, J.: 2005, *Astrophys. J.* **624**, 1057.
Régnier, S., Amari, T., Kersalé, E.: 2002, *Astron. Astrophys.* **392**, 1119.
Schrijver, C.J., Zwaan, C.: 2000, *Solar and Stellar Magnetic Activity*, *Cambridge Astrophysics Series* **34**, Cambridge University Press, Cambridge.
Schrijver, C.J., Derosa, M.L., Metcalf, T.R., Liu, Y., McTiernan, J., Régnier, S., Valori, G., Wheatland, M.S., Wiegelmann, T.: 2006, *Solar Phys.* **235**, 161.
Schwabe, M.: 1844, *Astron. Nachr.* **21**, 233.
Topka, K., Moore, R., Labonte, B.J., Howard, R.: 1982, *Solar Phys.* **79**, 231.
Wang, Y.-M., Nash, A.G., Sheeley, N.R. Jr.: 1989, *Science* **245**, 712.
Wang, Y.-M., Sheeley, N.R. Jr., Lean, J.: 2002, *Astrophys. J.* **580**, 1188.
Wang, Y.-M., Sheeley, N.R. Jr., Nash, A.G.: 1991, *Astrophys. J.* **383**, 431.
Wilmot-Smith, A.L., Hornig, G., Priest, E.R.: 2006, *Proc. Roy. Soc. Lond. Ser. A* **462**, 2877.
Zhang, M., Low, B.C.: 2001, *Astrophys. J.* **561**, 406.
Zhang, M., Low, B.C.: 2002, *Astrophys. J.* **576**, 1005.
Zhang, M., Low, B.C.: 2003, *Astrophys. J.* **584**, 479.